Nano Energy 90 (2021) 106517

Contents lists available at ScienceDirect

Nano Energy

journal homepage: www.elsevier.com/locate/nanoen

Artificial intelligence of toilet (AI-Toilet) for an integrated health monitoring system (IHMS) using smart triboelectric pressure sensors and image sensor

Zixuan Zhang [a,b], Qiongfeng Shi [a,b], Tianyiyi He [a,b], Xinge Guo [a,b], Bowei Dong [a,b], Jason Lee [c], Chengkuo Lee [a,b,d,*]

[a] Department of Electrical and Computer Engineering, National University of Singapore, 4 Engineering Drive 3, Singapore 117576
[b] Center for Intelligent Sensors and MEMS, National University of Singapore, Block E6 #05–11, 5 Engineering Drive 1, Singapore 117608
[c] EtooRex Pte. Ltd, 8 Circular Road, #02–01, Singapore 049422
[d] NUS Graduate School - Integrative Sciences and Engineering Programme (ISEP), National University of Singapore, Singapore 119077

ARTICLE INFO

Keywords:
Smart toilet
Triboelectric
Pressure sensor
Deep learning
AI-toilet

ABSTRACT

Smart toilet provides a feasible platform for the long-term analysis of person's health. Common solutions for identification are based on camera or radio-frequency identification (RFID) technologies, but it is doubted for privacy issues. Here, we demonstrate an artificial intelligence of toilet (AI-toilet) based on a triboelectric pressure sensor array offering a more private approach with low cost and easily deployable software. The pressure sensor array attached on the toilet seat is composed of 10 textile-based triboelectric sensors, which can leverage the different pressure distribution of individual users' seating manner to get the biometric information. 6 users can be correctly identified with more than 90% accuracy using deep learning. The signals from pressure sensors also can be used for recording the seating time on the toilet. The system integrates a camera sensor to analyze the simulated urine by comparing with urine chart and classify the types and quantities of objects using deep learning. All information including two-factor user identification and entire seating time using pressure sensor array, and data from the urinalysis and stool analysis were automatically transferred to a cloud system and were further shown in user's mobile devices for better tracking their health status.

1. Introduction

Recent advances in various sensor technologies have enabled cost-effective approaches for wireless network connectivity between various sensors and processors, which lead to visible progress in the Internet of Things (IoT) [1–5]. IoT, which consists of a large number of devices connected to the internet, is considered a promising technology for the consumer electronics market [6–8]. Therefore, with the development of 5G and IoT, smart homes are playing an increasingly important role in human life [9–12]. The eventual realization of smart home requires integrating considerable sensors with diversified functionalities distributed around the house to form a home network monitoring and managing the house environment [13–16]. In addition, current precision medicine is still mainly limited to disease treatment, rather than prevention and early detection. In this regard, smart home integrated with various sensors shows great potential in relevant healthcare applications [17–20]. The future smart home should achieve continuous health monitoring diagnostic information including various informative molecules, such as breath [21], sweat [22–24], urine [25,26], and stool [27,28], all of which are complex by-products of human systems, activities, and external environments. By leveraging various necessary sensors, smart home can provide valuable information for the health condition of individuals from these excreted matters [29–32]. Therefore, smart toilet could be the most effective platform for continuous health monitoring and valuable clinical information acquisition by analysing human excrement in smart home [33].

In the past few decades, several industrial manufacturers have attempted to build consumer-grade smart toilets. For an example, a Japanese company designed a smart toilet product [34], in which the main measurements are simple health status data, such as urine temperature, diet, body fat and weight, while these data are rarely available for clinical information. Unfortunately, its price is 6100 USD per set,

* Corresponding author at: Department of Electrical and Computer Engineering, National University of Singapore, 4 Engineering Drive 3, Singapore 117576.
E-mail address: elelc@nus.edu.sg (C. Lee).

https://doi.org/10.1016/j.nanoen.2021.106517
Received 7 July 2021; Received in revised form 3 September 2021; Accepted 11 September 2021
Available online 20 September 2021

which may not be affordable for ordinary households. In addition, other teams have introduced similar ideas and inventions for the realization of smart toilets in various forms [35–37]. These traditional smart toilets are based on facial recognition by camera sensor or RFID fingerprint recognition to record the individual health status. However, most of the toilets are placed in the bathroom, hence the recognition methods based on image sensors may cause privacy concerns for most users. The RFID fingerprint methods also need to consider the data security since fingerprints are commonly used as secure payment approach. Recently, there is another system which uses fingerprinting and anal creases (named as analprint) as biometric identifiers to securely associate the collected data with the user's identity [38]. Although this method can effectively protect the individual's biometrics information, it cannot be accepted by the majority of users. Moreover, even if this type of smart toilet integrates RFID for biometric identification, it usually also requires a pressure sensor as a switch to trigger the system and record the seating time and defecation time. Therefore, directly using the pressure sensor array for biometric identification can provide a better solution for user comfort and convenience [39–43]. In addition, method based on pressure sensor array can also record more comprehensive biometric information of the user seating on the toilet.

There have been a lot of biometric identification approaches through pressure sensor array, but most of them are based on piezoelectric sensors, capacitive sensors and resistive sensors [44–47]. Since most of these sensors are rigidly inflexible and unwashable, they are not suitable for placing on the toilet seat. There are several research developments of smart textiles aimed to be not only more comfortable but also multifunctional [48–51]. Benefiting from the particular advantages of various choices of materials, easy fabrication, self-power genenration, and low cost, the triboelectric nanogenerator (TENG) gradually becomes an optimal option based on textile format for sensors and energy harvesters [52–59]. Textile-based TENG (T-TENG) exhibits outstanding ability of structural retention and fatigue resistance during washing [60,61]. In addition, TENG has made a lot of research progress in various applications, including self-powered pressure sensor and human−machine interface (HMI) for IoT applications [62–70], and HMIs for robotic control and virtual/augmented reality (VR/AR) interactions [71–76]. However, the pressure sensor array based on triboelectric has not been used to achieve biometric identification because TENG is very susceptible to environmental variations resulting in reduced recognition accuracy. For decades, machine learning (ML) has provided an effective method to adaptively learn features from the collected raw signals. These features have achieved great results in image processing, speech recognition, human activity recognition, etc [77–80]. TENG signals are mainly generated as time series data with positive and negative peaks within the time of the whole motions. Therefore, advanced data analysis methods for triboelectric signals mainly use the AI algorithm based on the analysis of sequential data, such as CNN (convolutional neural network), RNN (recurrent neural network), LSTM (long short-term memory) and their combination [81–83]. There are some recognition tasks based on triboelectric sensor with the aids of deep learning, such as a smart glove for different hand gesture recognition using CNN [84], a smart keyboard for identification based on DBN (deep belief network) [85], and etc. Under the analysis of the DL (deep learning) algorithms, the basic characteristics of triboelectric sensor can be extracted, and the attention to unnecessary fluctuations such as signals changes in amplitude caused by humidity will be reduced [86–88]. Therefore, using TENG pressure sensor together with DL methods for biometric identification is desirable for the application of smart toilet, which can well protect the privacy of users while maintaining low cost and comfort.

In this work, we demonstrate an AI-toilet system equipped with multiple functions for an integrated health monitoring system (IHMS). The AI-toilet composed of a triboelectric pressure sensor array for biometrics identification and a commercial image sensor for healthcare monitoring. 10 textile-based triboelectric sensors with the aids of spacer and frustum structure on triboelectric layer can successfully extend the sensing range to detect the variation of pressure on toilet seat, offering a more private approach for identification in smart toilet with the advantages of low cost and easy fabrication. With the aids of DL, the biometrics information from 6 users sitting on the toilet seat can be identified with more than 90% accuracy. In addition, the signals from pressure sensors also can record the sitting time on the toilet. The recognition of simulated 4 different categories of stools and 5 amounts of stools reach the accuracy of 97.50% and 91.15%, respectively. Finally, all information about user's health status collected from the AI-toilet will be upload to server and further shown on user's mobile devices for continuous health monitoring and the valuable clinical information acquisition. The AI-toilet is capable of processing multi-modal data from the collected data on the hardware side to the AI interpretation on the software side, and finally can be combined with IoT to realize the AIoT system based on smart home (Fig. 1).

2. Results and discussion

2.1. Design, sensing mechanism and characterization

Our low-cost T-TENG sensors are created using a 3D printed mold to pattern the mm-scale frustum structure and a spacer on the silicone rubber surface (Fig. 2a; further details on characterization and preparation are provided in Fig. S1 and Experimental section). The T-TENG sensor contains four functional layers, including a nitrile thin film, a silicone rubber film, and two conductive textiles attached to the back of the two contact electrification layers for charge collection. Moreover, two non-conductive textile layers are used to seal the device on the outer surface. The working mechanism of the T-TENG sensor is contact-separation mode of TENG, where the pressure stimulus will induce charges to flow in the external circuit, and hence the mechanical energy can be transformed into electricity. There are a lot of works that prove adding a frustum structure to the surface of triboelectric layer of TENG will increase the sensing range [89–95]. But to better apply for the toilet seat, we design a T-TENG with a higher sensing range. Here we attempted three spacers with different heights (Fig. 2b). Although the output of the T-TENG sensor with spacer will decrease, the sensing range will correspondingly increase. When the height of spacer is 2 mm, the buffering effect for pressure is relatively small due to the low height, hence the output is reduced less, and the sensing range is hardly improved. However, when the spacer height is 5.5 mm, although the sensing range is increased to 300 kPa, its output is only half of that without the spacer. If the output is too low, the resolution of the subsequent ADC sampling will be greatly disturbed. Therefore, we chose the T-TENG sensors with medium-height spacer. When the height of the spacer and frustum is 4 mm, the sensing range can be successfully expanded to more than 200 kPa. The detailed dimensions of T-TENG sensor with 4-mm spacer and frustum structure are shown in Fig. 2c. Without the specific illustration, the frustum-patterned sensor with 4 mm height spacer is used for all the following testing and demonstrations. As for the stretching stability, since the sensor is put under 1000 N which undergoes negligible lateral strain but large normal pressure, the repetitive contact-separation process resembles the real situation quite well. To further verify durability and reproducibility, we measured the open circuit responses of the pressure sensor under 400 kPa over 500 cycles (Fig. 2d). The open-circuit response of the pressure sensor was stable and regular, with an almost constant base voltage. These results show that the proposed T-TENG sensors can reliably collect seating signals as biometrics identification element applied for smart toilet system.

2.2. Individual pressure distribution

Because the proposed T-TENG has good stability and durability, we put ten T-TENG sensors on the toilet as a pressure sensor array to detect the different pressure distributions of different users when they sit on the

Fig. 1. The schematics of Artificial Intelligence of Toilet (AI-Toilet) using triboelectric pressure sensors and image sensor for integrated health monitoring system (IHMS) as an important component of smart home applications.

toilet, as shown in Figs. 3a and S2. In order to realize the further IoT application, we use a microcontroller unit (Arduino mega 2560) and a customized PCB to realize analogue to digital convert (ADC) function. The voltage value of T-TENG collected by this method will be converted into a value between (0 V, 5 V). Due to the existence of the voltage divider circuit, the zero value of the T-TENG signal will be set to around 3.35 V. Hence the voltage range that can be detected is (−3.35 V, 1.65 V). When the user sits on the toilet seat, according to the contact-separation mechanism of TENG, eco-flex layer as a negative triboelectric layer will get electrons, and the ADC will detect a negative voltage (Fig. 3b). When leaving the toilet seat, a positive voltage value will be correspondingly detected. Considering that the general composition of family members is six, hence we first consider the individual recognition under six people. Therefore, we selected 6 users (male: User 1, User 2, User 4, and User 6; female: User 3 and User 5) to sit on the toilet seat in a normal state and leave the toilet after keeping 10 s of stability. As shown in Fig. 3c, different users have different habits to sit on different positions and produce different pressures. For better visualizing the pressure distribution map, we take the peak value of each channel from the entire waveform generated during the sitting process of the user and compare it with the detectable maximum voltage value. The pressure distribution of almost all participants is mainly concentrated in Sensor 1, Sensor 2, Sensor 3, Sensor 6, Sensor 7 and Sensor 8, which indicates the main pressure distribution area for most people sitting on the toilet. In addition, the pressure map of two female participants User 3 and User 5 shows that the position of Sensor 4, Sensor 5, Sensor 9 and Sensor 10 are almost completely unused. Besides, the habit of 6 users sitting on the toilet is quite different, causing each user have the different distribution of pressure when sitting on the toilet. Meanwhile, we collected data from six users 50 times for verifying the stability of seating signal from individuals. As shown in Fig. 3d, the 50 times sitting pressure distributions of User 6 are similar, and there is a relatively large difference compared to other users (Fig. S3).

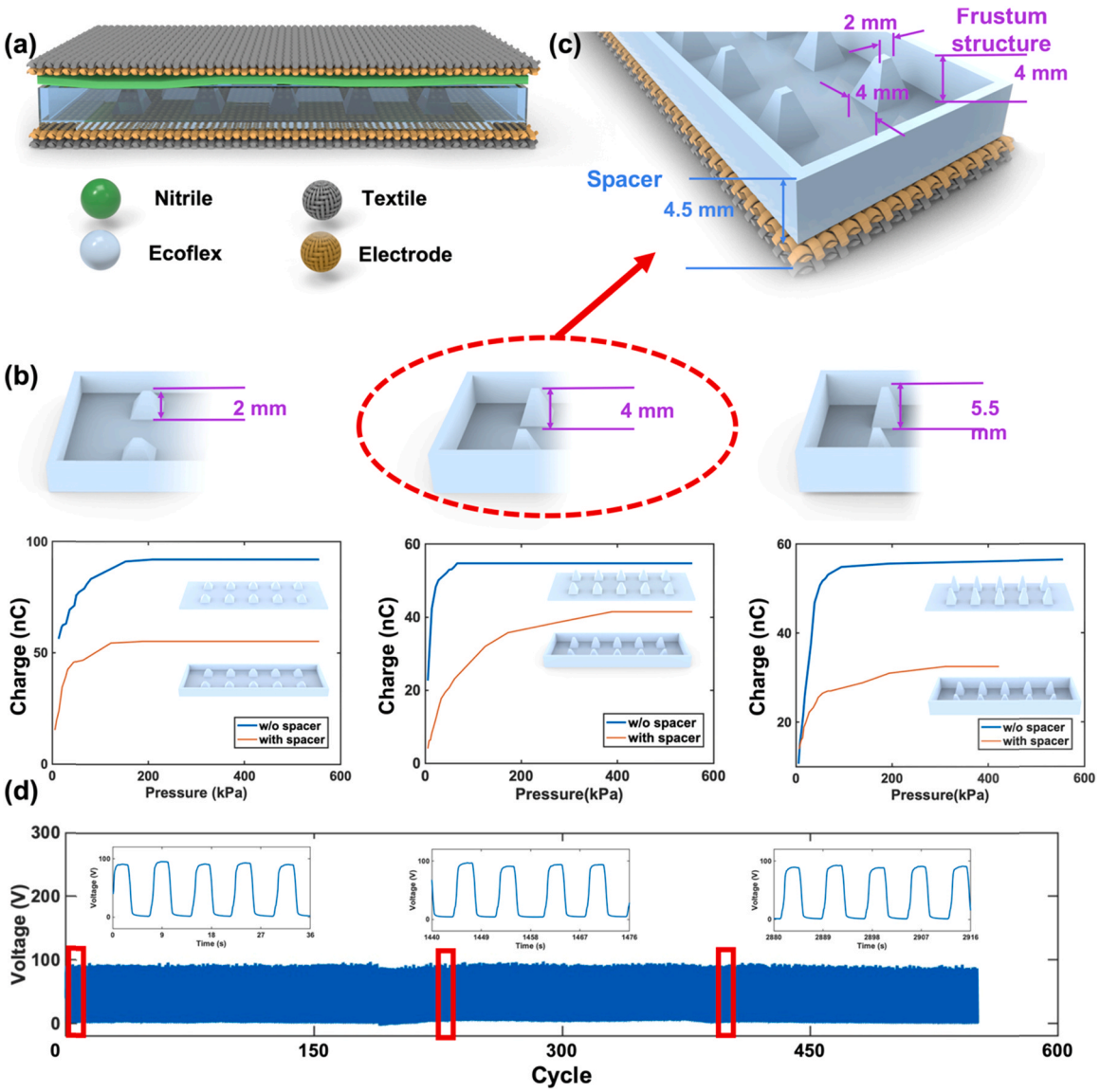

Fig. 2. (a) Schematic diagram of the textile-based triboelectric sensor (T-TENG). (b) The charge versus pressure curve of frustum-based T-TENG with spacer structure and without spacer structure under the height of 2 mm, 4 mm, and 5.5 mm. (c) The detailed dimensions of the 4 mm-frustum and spacers. (d) The stable performance of a T-TENG over 500 cycles under the load of 400 kPa.

2.3. Biometrics identification

The traditional triboelectric device analysis strategy is to manually extract shallow features from a single waveform, such as frequency, hold time, and peak gap, which cannot realize the recognition of complex features [96–98]. These features have subtle differences and are very susceptible to environmental changes. The impact of these methods will led to a reduction in recognition accuracy. Therefore, it is difficult to directly use the pressure sensor distribution map extracted before for biometric identification. Due to the high performance of DL on dealing with many types of data, DL has become a very popular subset of ML. Triboelectric signal is usually recorded as one-dimensional (1D) time-series or discrete data, hence AI algorithm provide a promising and feasible solution for analysis of the time-series data [99–102]. Compared with manually extracting features, various AI algorithms also have capability of saving human resources and performing various classification problems more conveniently and concisely. Therefore, as shown in Fig. 4a, a three-layer 1D-CNN was then constructed for data feature extraction and automatic recognition to verify the sensing ability of the proposed AI-toilet system. The detailed parameters of the ML architecture can be found in experiment section.

In addition to the previous 50 samples of each users are setting as training set, the new 10 data samples of each users are collected as test set. The data length for each channel is 150, so there are 10 channels × 150 = 1500 features in total for each sample as the input of the 1D-CNN analytic. Firstly, the t-distributed stochastic neighbor embedding (t-SNE) algorithm as a nonlinear dimensionality reduction technique is well suited for embedding high-dimensional data for visualization in a low-dimensional space of two or three dimensions, which is successfully utilized to visualize the clustered results of the data set, as shown in Fig. 4b. To achieve better performance for classification, the whole data is firstly zero-centered and rescaled to [−1, 1] before algorithm training. As shown in Fig. 4c, the 1D CNN actually achieve high test accuracy rate by accident that it is the only time to achieve the 97.41% accuracy on the test data. The training process of accuracy rate versus iteration time on the train set validation set and test set are shown in Fig. S4. The real-time demonstration of identification is shown in Video S1. For the time sequence signal, the RNN, LSTM and 1D CNN are the classical algorithm which is also tested. SVM, as a kind of strong classification algorithm, is also considered for comparing the performance of different algorithms.

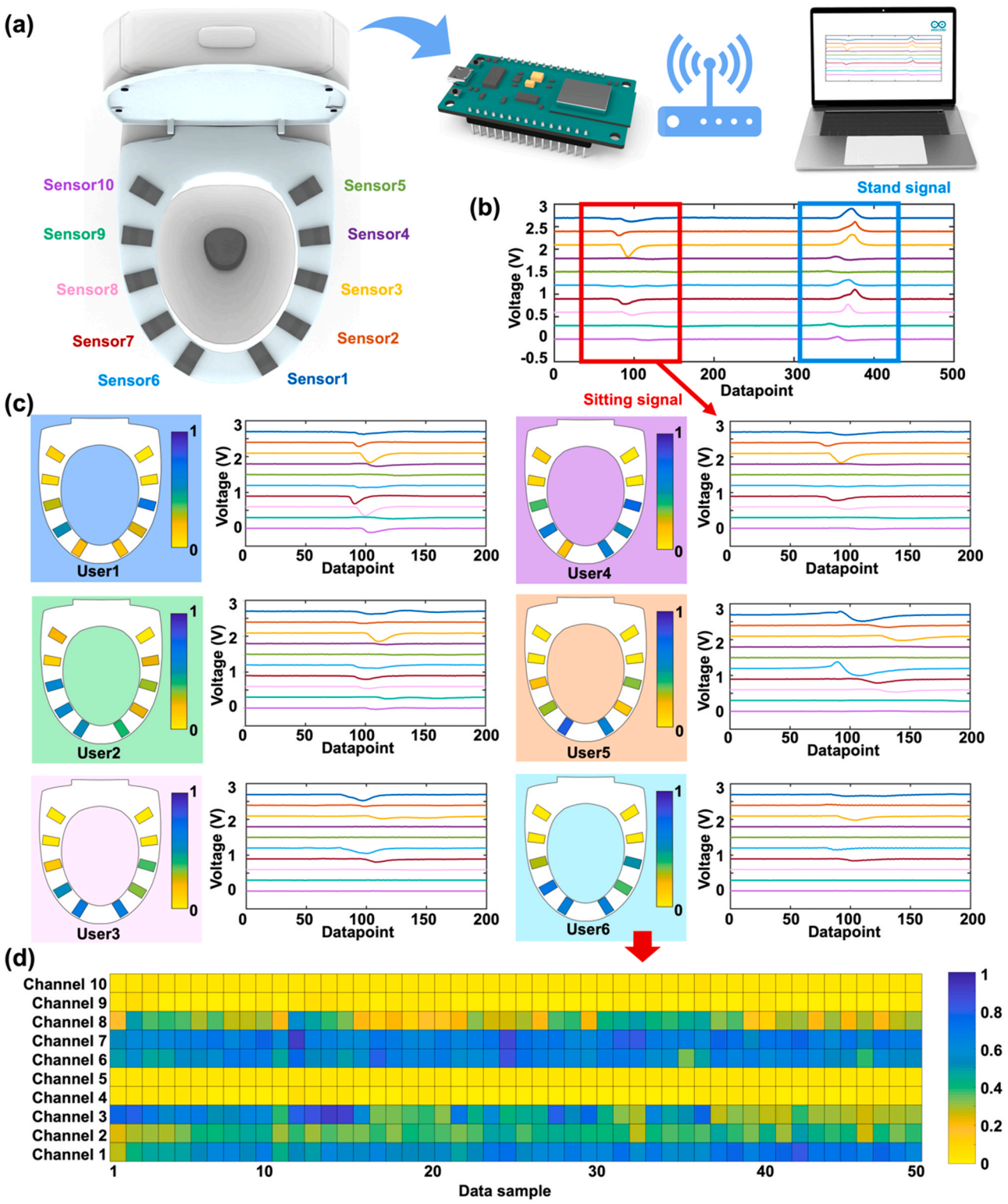

Fig. 3. (a) Schematics of the data acquisition system to collect sensory information of sitting signal and stand signal. (b) The sensor signal from 10 T-TENG sensors after ADC. (c) The sitting signals of six different users and the converted pressure distribution maps. (d) The pressure distribution map of 50 sets of cushion signals collected from User 6.

The results of 2D CNN, RNN, LSTM, SVM, and 1D CNN has been shown in Table S1. It is clear that the 1D CNN can achieve the highest accuracy and the SVM and RNN can also obtain an acceptable generalization ability for six individual recognitions on 10 sensors. In order to obtain the influence of the number of triboelectric sensors and their positions on the accuracy of CNN, we test the performance of 1D CNN based on two sensors (3, 8), four sensors (1, 3, 6, 8), six sensors (1, 3, 5, 6, 8, 10), eight sensors (1, 2, 3, 5, 6, 7, 8, 10) and ten sensors (1, 2, 3, 4, 5, 6, 7, 8, 9, 10) in Fig. 4d. It is worthy to mention that with the increase of sensor number, the generalization ability of all kinds of algorithms will increase. In addition, increasing the number of sensors can benefit to improve algorithm performance that the learning speed can be

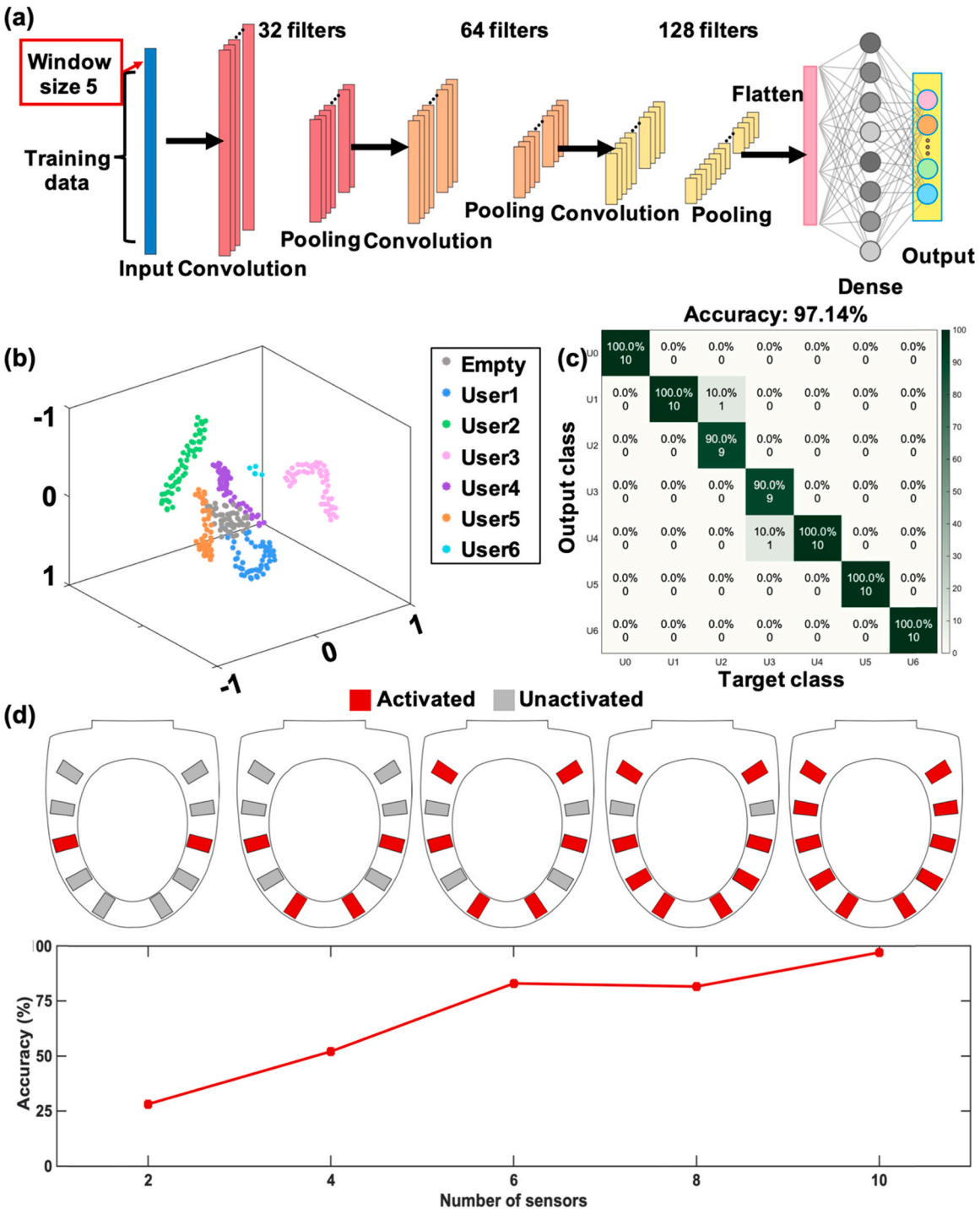

Fig. 4. (a) Schematics of the process and parameters for constructing the 1D CNN structure. (b) t-SNE plot from our sitting pose dataset recorded by the pressure sensor array. (c) Confusion map of the prediction with the sitting signals of 6 participants. (d) Schematic diagram of the sensor distribution and accuracy rate of different numbers of sensors.

expedited, and generalization ability will be enhanced. As shown in Fig. S5, the classification results of 10 people can reach the accuracy of 94.55%. In the future, if more individual is required to be recognized, applying more triboelectric sensors for improving performance is reasonable.

Supplementary material related to this article can be found online at doi:10.1016/j.nanoen.2021.106517.

2.4. Image recognition

In our AI-toilet system, the function of urine and stool state evaluation is achieved by analysis the captured photo image. The system graphical is illustrated in the Fig. 5a. Based on the image sensor embedded on an AIoT module (MaixDuino board), the images inside the toilet can be captured for ulterior analysis. The collected images will be directly transmitted to the microprocessors where the trained machine learning algorithms have been recorded on. Based on the fitted algorithm and transmitted image, the AIoT module will directly generate the

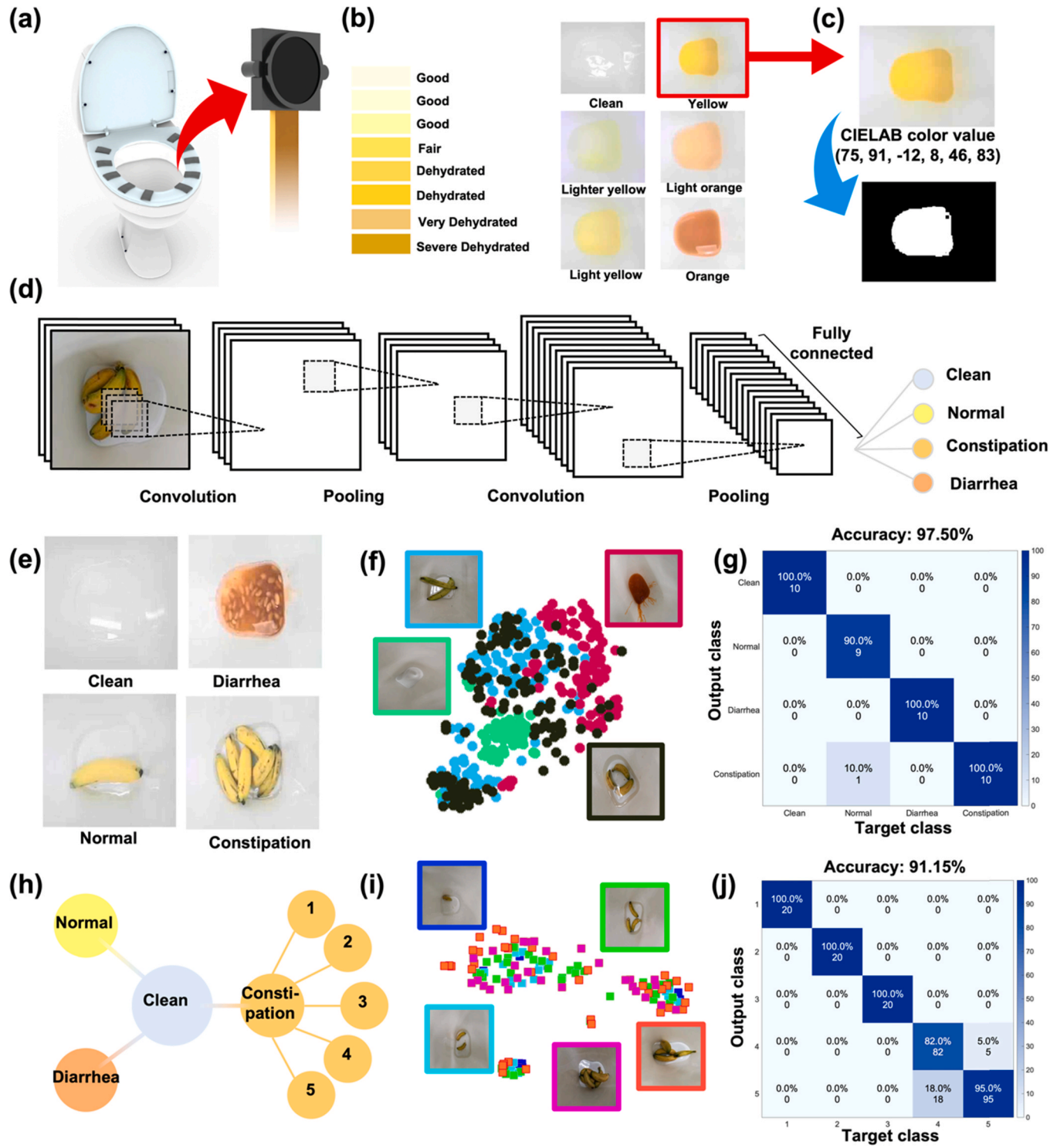

Fig. 5. (a) Schematic diagram of commercial image sensor. (b) Common urine chat and simulated urine diagrams used in experiments. (c) The designated color area map obtained by setting the threshold of CIELAB. (d) Layout of used deep CNN structure for classification of stool states. (e) Simulated stool states of four toilets. (f) t-SNE visualization of the last hidden-layer representations in the CNN for four stool classes. (g) The confusion map for CNN outcome of 4 simulated stool states. (h) A schematic of the simulated stool taxonomy and number. (i) The t-SNE visualization of the last hidden-layer representations in the CNN for 5 types of constipation stool. (j) The confusion map for CNN outcome of 5 simulated constipation stool states.

output result, which means all the image process have been integrated into a single chip. Firstly, the urine color detection is achieved based on lab color space (LAB). Different color has different threshold of LAB value, which is composed of many pixels and each pixel has its certain LAB value. By estimating and comparing the number of pixels in the certain LAB range, it is possible to obtain the main color components of the image. The image from the toilet will be gathered and transmitted into AIoT module where the number of pixels of each color is calculated. In order to simulate the urine chat which can recognize the preliminary health status through define different fixed color, here six different colors are selected for the simulation of urinalysis in Fig. 5b. As shown in Fig. 5c, the LAB range of 'yellow' is considered as (75, 91, −12, 8, 46,

83), which means: (minimum L, maximum L, minimum A, maximum A, minimum B, maximum B). It means that the pictures captured by the camera will be divided according to the interval of the three set values of LAB, the pixels in the interval are white, and the others are black. Similarly, as shown in Fig. S6, the LAB range of 'white' is considered as (90, 94, −3, 6, −13, 3), the LAB range of 'lighter yellow' is considered as (83, 92, −15, −1, 4, 32), the LAB range of 'light yellow' is considered as (83, 92, −15, −3, 32, 48), the LAB range of 'light orange' is considered as (77, 88, 1, 16, 17, 37) and the LAB range of 'orange' is considered as (58, 78, 21, 33, 29, 43), respectively. Since the toilet itself is white, it is necessary to subtract a specific value from the number of white pixels to ensure that the recorded number of white pixels is only the area at the middle area which we are concerned about. In an addition, when the number of pixels of all colors is less than a threshold value, it will be determined as a new kind of color represents the image and output result as 'undefined color'.

Image sensor also can be used to achieve the function of stool recognition. Based on the characteristics of each category, three categories of excreta based on other succedaneum are achieved. Here we used baked beans in tomato sauce to simulate the diarrhea start of stool, and bananas of different sizes to simulate the normal state and constipation state of stool, as shown in Fig. 5e. CNN has always been considered to have a strong advantage in image processing. As shown in Fig. 5d, the utilized CNN structure in AI-toilet includes 2 convolutional layers, 1 max pooling layer and 1 fully connected layer. The output of CNN is four which corresponding to the categories of four different

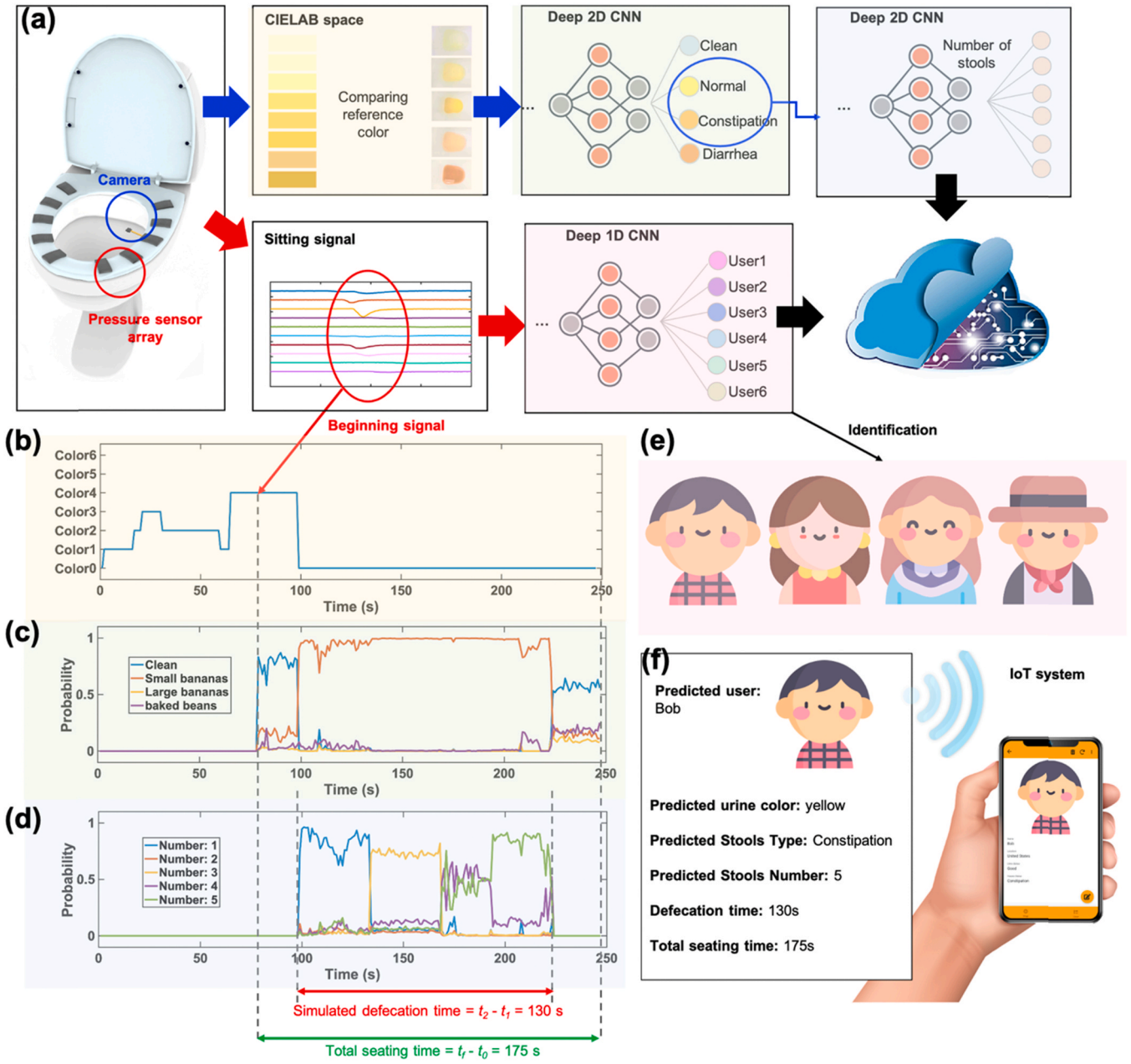

Fig. 6. (a) Schematic of the whole functions of IHMS, including urine detection, type and number recognition of stool state, seating time and defecation time recording, user identification and IoT application. (b) An example graph of image sensor detecting the results of simulated urine. When the seating signal is triggered, the image sensor turns on CNN for stool recognition. (c) The probability of the first custom CNN to judge the type of tool. (d) If the toilet status is constipation, then the images are introduced into the second custom CNN to determine their number. (e) The seating signal is also collected for identification. (f) All information will be uploaded to the cloud through the PC, and then transmitted to the user's mobile phone through the cloud.

states. For each type of data set, the data has been separated into training set (80%) and validation set (20%) for algorithm training. The training data is used to verify whether algorithm is underfitting and the validation data is applied to check whether it is overfitting. Finally, the accuracy of CNN is 97.50% and the confusion map is shown in Fig. 5g, which also shows that the difficulties of algorithm mainly focus on the recognizing of normal and constipation. Image recognition is usually affected by the dark environment, here we also proposed data augmentation methods to improve the performance of CNN, as shown in Fig. S7. There are six kinds of data set to verify the performance of data augmentation technology. As shown in Table S2, position change can increase the correct rate to 83.82%. The position change operation will be a better choice as it almost does not lose any information or add disturbing information. As illustrated in Fig. 5h, when the constipation condition is appeared, the image will be transmitted to another CNN algorithm to detect the number of this category. As elaborated in the Fig. 5i, t-SNE visualizes the two features from five different classes for number recognition. The confusion matrix of test data is illustrated in the Fig. 5i, which can get the accuracy of 91.15%. The class four and class five are easy to be confounded due to the overlap of increasing objects.

2.5. Integrated AIoT system

After integrating the above functions, the AI-toilet based on image sensor and T-TENG can then realize the AIoT application on smart home, as shown in Fig. 6a and Video S2. AI-toilet will perform simple color recognition first and then compare with the urine color chart to get the user's water shortage and preliminary health status. As shown in Fig. 6b, the urine state is simulated by adding liquid to the toilet. It can be seen that the simulated color changed from color0 (undefined color) to color1 (white), and eventually became color4 (yellow) as the juice concentration increased. After stopping changing the color, the output result will remain at color4. When the pressure sensor receives a trigger signal, the image recognition function is turned on. The neural network for excrement classification that has been burned on AIoT module will be activated first. When the stimulated defecation process starts by placing a small banana in the AI-toilet, the CNN will differentiate it as the stool state. At the same time, the LAB-based color recognition function is turned off. As shown in Fig. 6c and d, between 80 and 100 s, the probability of judging as clean is greater than 80% on average, so it can be judged that the banana has not been placed during this period. After 100 s, the system detects the occurrence of small bananas (i.e., simulated constipation) and turns on the neural network for identifying the number of objects at the same time. As the number of small bananas increases, the result of object classification gradually approaches 100%, and the corresponding probability distribution will be obtained for the number detection. After all the small bananas are finally removed, when the probability of clean in the result of object recognition is also the highest, the neural network for quantitative recognition will not be activated again. The period from the first detection of the appearance of the small banana (t_1) to the new detection of clean (t_2) can be regarded as the simulated defence time. The pressure sensor signal can be detected as trigger signal to record the beginning of seating (t_0). As the T-TENG based pressure sensor detects the departure signal (t_f), the total seating time can be obtained through t_f-t_0. At the same time, all data during this period, including urine color, excrement image recognition, excrement quantity and the corresponding time will be uploaded to the local PC. On the other hand, when the pressure sensor signal is detected at the beginning, the data of 10 pressure sensors will be also used to obtain the predicted user's identity information through the 1DCNN. In the end, all information will be uploaded to the cloud through the PC, and then transmitted to the user's mobile phone through the cloud. Therefore, it not only protects the privacy of users, but also allows family members to better pay attention to the health of elder or children. Therefore, the proposed smart toilet will obtain various types of health information after interpreting the state and habits of the user, thereby realizing disease detection, whose intelligence and versatility will become one of the final solutions of smart toilets in smart home.

Supplementary material related to this article can be found online at doi:10.1016/j.nanoen.2021.106517.

3. Conclusion

In general, an AI-toilet for IHMS based on a triboelectric pressure sensor array for biometrics identification and a commercial image sensor for urinalysis and stool analysis is developed. Leveraging the frustum structure on eco-flex layer and spacer between two triboelectric layers, the sensing range successfully extends up to above 200 kPa, which is suitable for detection of seating pressure. 10 textile-based triboelectric sensors as a pressure sensor array are attached on the toilet seat, offering a more private approach with the advantages of low cost and easy fabrication. With the aids of DL, the biometrics information from 6 users seating on the toilet seat can be identified with more than 90% accuracy. In addition, the signals from pressure sensors also can record the seating time of toilet. We used an image sensor of an AIoT module to record the dynamic variation of color within the toilet, and to realize the urinalysis. CNNs have been applied successfully in visual recognition tasks such as image classification. Therefore, we design two CNNs for the recognition of simulated 4 different types of stools and stools' amounts with accuracy of 97% and 91%, respectively. Finally, all information about user's health status collected from smart toilet system will be uploaded to server and further shown on user's mobile devices for continuous health monitoring and the valuable clinical information.

4. Experimental section

4.1. Fabrication of the triboelectric textile sensor

The triboelectric textile sensor contains two layers: a positive charge generation layer, and a negative charge generation layer. Firstly, the conductive textile is cut into the desired size and shape, which is made of metalized fabric (polyester Cu) coated with an adhesive. To fabricate the positive charge generation layer, a thin nitrile film is attached to one side of a conductive textile. Another conductive textile is coated with silicone rubber film on the one side as well (Fig. S1). The coating process was firstly dispensing required amounts of Parts A and B of the Eco-FlexTM 00–30 into a mixing container (1 A:1B by volume or weight), followed by mixing the blend thoroughly for 3 min, and then the mixed solution was poured into a 3D-printed mold followed by 20-minute baking at 40 ºC for curing. Lastly, the silicone rubber coated textile was stitched to the nitrile coated textile with two non-conductive textiles attached to the outer sides for encapsulation.

4.2. Experiment measurement and characterization

The signal outputs in the characterization of the textile-based TENG sensor were measured by an oscilloscope (DSO-X3034A, Agilent) using a high impedance probe of 100 MΩ. Calibrations of output voltage against force for triboelectric sensors were conducted by force gauge (Mecmesin, MultiTest 2.5-i) with the speed of 600 mm/min. The open-circuit voltages, transferred charges, and short-circuit currents were measured by an electrometer (Model 6514, Keithley), and the signals were displayed and recorded by an oscilloscope (DSO-X3034A, Agilent).

4.3. Data acquisition and data analysis

Analog voltage signals generated from T-TENG are collected and processed by the hardware circuit consisting of a conditioner print circuit board (PCB) and an MCU (Arduino Mega 2560). After the measurements, MATLAB®2019a was used for data analysis. The 1D CNN models were developed in Python with Keras and Tensorflow backend.

The proposed 1D CNN architecture includes three convolutional layers with 16, 32, and 64 filters and a kernel size of 5 × 5, each of them followed by a max-pooling layer. Image analysis based on AIoT module (Sipeed Maixduino) based on kendryte K210 risc-v AI processor, Arduino uno and on-board esp32 WIFI, Bluetooth module and M1 AI module. MaixPy IDE 0.2.5 help to use the micro-python to realize WIFI connection, computer vision and machine learning on the MaixDuino board.

CRediT authorship contribution statement

Zixuan Zhang: Conceptualization, Methodology, Software, Validation, Data curation, Formal analysis, Investigation, Visualization, Writing – original draft, Writing – review & editing. **Qiongfeng Shi:** Conceptualization, Methodology, Software, Validation, Data curation, Formal analysis, Investigation, Visualization, Writing – original draft, Writing – review & editing. **Tianyiyi He:** Methodology, Formal analysis, Investigation, Writing – review & editing. **Xinge Guo:** Methodology, Formal analysis, Investigation. **Bowei Dong:** Methodology, Formal analysis, Investigation. **Jason Lee:** Conceptualization, Methodology, Formal analysis, Investigation. **Chengkuo Lee:** Conceptualization, Methodology, Investigation, Writing – review & editing, Supervision, Project administration, Funding acquisition.

Declaration of Competing Interest

The authors declare that they have no known competing financial interests or personal relationships that could have appeared to influence the work reported in this paper.

Acknowledgments

This work was partly supported the National Key Research and Development Program of China (Grant No. 2019YFB2004800, Project No. R-2020-S-002) at NUSRI, Suzhou, China; and NAMIC funding of Fast Prototyping of Smart Toilet IoT Sensor System Using 3D Printing, Singapore (WBS: R-263–000-E54–592) at NUS, Singapore. This work is also thankful for the support from Mr. Dingbang Liu in the help of utilization of AIoT module, and CISM's members in the data collection part.

Appendix A. Supporting information

Supplementary data associated with this article can be found in the online version at doi:10.1016/j.nanoen.2021.106517.

References

[1] J. Xu, Z. Ren, B. Dong, X. Liu, C. Wang, Y. Tian, C. Lee, Nanometer-scale heterogeneous interfacial sapphire wafer bonding for enabling plasmonic-enhanced nanofluidic mid-infrared spectroscopy, ACS Nano 14 (2020) 12159–12172, https://doi.org/10.1021/acsnano.0c05794.
[2] Y. Zeng, P.H. Pathak, P. Mohapatra, WiWho: WiFi-Based Person Identification in Smart Spaces, 2016 15th ACM/IEEE Int. Conf. Inf. Process. Sens. Networks, IPSN 2016 - Proc., 2016. https://doi.org/10.1109/IPSN.2016.7460727.
[3] H. Liu, H. Fu, L. Sun, C. Lee, E.M. Yeatman, Hybrid energy harvesting technology: From materials, structural design, system integration to applications, Renew. Sustain. Energy Rev. (2020), 110473, https://doi.org/10.1016/j.rser.2020.110473.
[4] J. Zhu, X. Liu, Q. Shi, T. He, Z. Sun, X. Guo, W. Liu, O. Bin Sulaiman, B. Dong, C. Lee, Development trends and perspectives of future sensors and MEMS/NEMS, Micromachines 11 (2020), https://doi.org/10.3390/mi11010007.
[5] Q. Zhang, S. Zuo, P. Chen, C. Pan, Piezotronics in two-dimensional materials, 2021: 1–21. https://doi.org/10.1002/inf2.12220.
[6] X. Guo, L. Liu, Z. Zhang, S. Gao, T. He, Q. Shi, C. Lee, Technology evolution from micro-scale energy harvesters to nanogenerators, J. Micromech, Microeng. 31 (2021), 093002, https://doi.org/10.1088/1361-6439/ac168e.
[7] A.P. Plageras, K.E. Psannis, C. Stergiou, H. Wang, B.B. Gupta, Efficient IoT-based sensor BIG Data collection–processing and analysis in smart buildings, Futur. Gener. Comput. Syst. 82 (2018) 349–357, https://doi.org/10.1016/j.future.2017.09.082.
[8] K.R.S.D. Gunawardhana, N.D. Wanasekara, R.D.I.G. Dharmasena, Towards truly wearable systems: optimizing and scaling up wearable triboelectric nanogenerators, IScience 23 (2020), 101360, https://doi.org/10.1016/j.isci.2020.101360.
[9] R. Sokullu, M.A. Akkaş, E. Demir, IoT supported smart home for the elderly, Internet Things 11 (2020), 100239, https://doi.org/10.1016/j.iot.2020.100239.
[10] M. Jethanandani, A. Sharma, T. Perumal, J.-R. Chang, Multi-label classification based ensemble learning for human activity recognition in smart home, Internet Things 12 (2020), 100324, https://doi.org/10.1016/j.iot.2020.100324.
[11] X. Zhao, H. Askari, J. Chen, Nanogenerators for smart cities in the era of 5G and Internet of Things, Joule 5 (2021) 1391–1431, https://doi.org/10.1016/j.joule.2021.03.013.
[12] L. Liu, X. Guo, C. Lee, Promoting smart cities into the 5G era with multi-field Internet of Things (IoT) applications powered with advanced mechanical energy harvesters, Nano Energy., n.d.
[13] L. Wang, T. Gu, X. Tao, H. Chen, J. Lu, Recognizing multi-user activities using wearable sensors in a smart home, Pervasive Mob. Comput. 7 (2011) 287–298, https://doi.org/10.1016/j.pmcj.2010.11.008.
[14] B. Dong, Q. Shi, Y. Yang, F. Wen, Z. Zhang, C. Lee, Technology evolution from self-powered sensors to AIoT enabled smart homes, Nano Energy 79 (2021), 105414, https://doi.org/10.1016/j.nanoen.2020.105414.
[15] Q. Shi, Z. Zhang, T. He, Z. Sun, B. Wang, Y. Feng, X. Shan, B. Salam, C. Lee, Deep learning enabled smart mats as a scalable floor monitoring system, Nat. Commun. 11 (2020) 4609, https://doi.org/10.1038/s41467-020-18471-z.
[16] Q. Zheng, M. Peng, Z. Liu, S. Li, R. Han, H. Ouyang, Y. Fan, C. Pan, W. Hu, J. Zhai, Z. Li, Z.L. Wang, Dynamic real-time imaging of living cell traction force by piezo-phototronic light nano-antenna array, Sci. Adv. 7 (2021) 1–9, https://doi.org/10.1126/sciadv.abe7738.
[17] Q. Shi, C. Lee, Self-powered bio-inspired spider-net-coding interface using single-electrode triboelectric nanogenerator, Adv. Sci. 6 (2019), 1900617, https://doi.org/10.1002/advs.201900617.
[18] J. Huang, X. Yang, J. Yu, J. Han, C. Jia, M. Ding, J. Sun, X. Cao, Q. Sun, Z. L. Wang, A universal and arbitrary tactile interactive system based on self-powered optical communication, Nano Energy 69 (2020), 104419, https://doi.org/10.1016/j.nanoen.2019.104419.
[19] M. Zhu, Q. Shi, T. He, Z. Yi, Y. Ma, B. Yang, T. Chen, C. Lee, Self-powered and self-functional cotton sock using piezoelectric and triboelectric hybrid mechanism for healthcare and sports monitoring, ACS Nano 13 (2019) 1940–1952, https://doi.org/10.1021/acsnano.8b08329.
[20] C. Qiu, F. Wu, C. Lee, M.R. Yuce, Self-powered control interface based on Gray code with hybrid triboelectric and photovoltaics energy harvesting for IoT smart home and access control applications, Nano Energy 70 (2020), 104456, https://doi.org/10.1016/j.nanoen.2020.104456.
[21] A. Krilaviciute, J.A. Heiss, M. Leja, J. Kupcinskas, H. Haick, H. Brenner, Detection of cancer through exhaled breath: a systematic review, Oncotarget 6 (2015) 38643–38657, https://doi.org/10.18632/oncotarget.5938.
[22] L.B. Baker, J.B. Model, K.A. Barnes, M.L. Anderson, S.P. Lee, K.A. Lee, S. D. Brown, A.J. Reimel, T.J. Roberts, R.P. Nuccio, J.L. Bonsignore, C.T. Ungaro, J. M. Carter, W. Li, M.S. Seib, J.T. Reeder, A.J. Aranyosi, J.A. Rogers, R. Ghaffari, Skin-interfaced microfluidic system with personalized sweating rate and sweat chloride analytics for sports science applications, Sci. Adv. 6 (2020) 17–19, https://doi.org/10.1126/sciadv.abe3929.
[23] A.J. Bandodkar, S.P. Lee, I. Huang, W. Li, S. Wang, C.J. Su, W.J. Jeang, T. Hang, S. Mehta, N. Nyberg, P. Gutruf, J. Choi, J. Koo, J.T. Reeder, R. Tseng, R. Ghaffari, J.A. Rogers, Sweat-activated biocompatible batteries for epidermal electronic and microfluidic systems, Nat. Electron. 3 (2020) 554–562, https://doi.org/10.1038/s41928-020-0443-7.
[24] J.C. Yang, J. Mun, S.Y. Kwon, S. Park, Z. Bao, S. Park, Electronic skin: recent progress and future prospects for skin-attachable devices for health monitoring, robotics, and prosthetics, Adv. Mater. 31 (2019), 1904765.
[25] S. He, J. Li, Y. Lyu, J. Huang, K. Pu, Near-infrared fluorescent macromolecular reporters for real-time imaging and urinalysis of cancer immunotherapy, J. Am. Chem. Soc. 142 (2020) 7075–7082, https://doi.org/10.1021/jacs.0c00659.
[26] X. He, Q. Pei, T. Xu, X. Zhang, Smartphone-based tape sensors for multiplexed rapid urinalysis, Sens. Actuators B: Chem. 304 (2020), 127415, https://doi.org/10.1016/j.snb.2019.127415.
[27] M. Gaur, A. Singh, V. Sharma, G. Tandon, A. Bothra, A. Vasudeva, S. Kedia, A. Khanna, V. Khanna, S. Lohiya, M. Varma-Basil, A. Chaudhry, R. Misra, Y. Singh, Diagnostic performance of non-invasive, stool-based molecular assays in patients with paucibacillary tuberculosis, Sci. Rep. 10 (2020) 1–8, https://doi.org/10.1038/s41598-020-63901-z.
[28] R.J. Davies, R. Miller, N. Coleman, Colorectal cancer screening: Prospects for molecular stool analysis, Nat. Rev. Cancer 5 (2005) 199–209, https://doi.org/10.1038/nrc1569.
[29] F. Wen, Z. Zhang, T. He, C. Lee, AI enabled sign language recognition and VR space bidirectional communication using triboelectric smart glove, Nat. Commun. 12 (2021), 5378, https://doi.org/10.1038/s41467-021-25637-w.
[30] S. Gao, T. He, Z. Zhang, H. Ao, H. Jiang, C. Lee, A motion capturing and energy harvesting hybridized lower-limb system for rehabilitation and sports applications, Adv. Sci. 2101834 (2021) 1–16, https://doi.org/10.1002/advs.202101834.
[31] X. Guo, T. He, Z. Zhang, A. Luo, F. Wang, E.J. Ng, Y. Zhu, H. Liu, C. Lee, Artificial intelligence-enabled caregiving walking stick powered by ultra-low-frequency human motion, ACS Nano (2021), acsnano.1c04464, https://doi.org/10.1021/acsnano.1c04464.
[32] D. Vera, L. Chengkuo, K. Zhan, L. Tao, M.R. Yuce, T. Alan, Achieving non-contact monitoring of human activity using triboelectric sensing: enabling new assistive applications for the elderly and the visually impaired, Nano Energy (2021).

[33] V. Lohan, R.P. Singh, Home automation using Internet of Things, Lect. Notes Netw. Syst. 39 (2019) 293–301, https://doi.org/10.1007/978-981-13-0277-0_24.
[34] P.E. Hindenburg, Toilet device with health examination system, 1990.
[35] V. Mithya, N. Divya Prabha, S. Sisma Samlein, M. Madhumitha, Smart toilets using turbidity sensor, Int. J. Innov. Technol. Explor. Eng. 8 (2019) 413–417.
[36] A. Lokman, R.K. Ramasamy, Smart toilet: Threats and challenges identifying human presence using iot sensors, ACM Int. Conf. Proceeding Ser., 2019: 56–60. https://doi.org/10.1145/3361758.3361765.
[37] S. Hashemi, M. Han, T. Kim, Y. Kim, Innovative Toilet Technologies for Smart and Green Cities, 2015: 873–879. https://doi.org/10.3390/ifou-e013.
[38] S. min Park, D.D. Won, B.J. Lee, D. Escobedo, A. Esteva, A. Aalipour, T.J. Ge, J. H. Kim, S. Suh, E.H. Choi, A.X. Lozano, C. Yao, S. Bodapati, F.B. Achterberg, J. Kim, H. Park, Y. Choi, W.J. Kim, J.H. Yu, A.M. Bhatt, J.K. Lee, R. Spitler, S. X. Wang, S.S. Gambhir, A mountable toilet system for personalized health monitoring via the analysis of excreta, Nat. Biomed. Eng. 4 (2020) 624–635, https://doi.org/10.1038/s41551-020-0534-9.
[39] X. Ran, C. Wang, Y. Xiao, X. Gao, Z. Zhu, B. Chen, A portable sitting posture monitoring system based on a pressure sensor array and machine learning, Sens. Actuators A: Phys. 331 (2021), 112900, https://doi.org/10.1016/j.sna.2021.112900.
[40] B.W. An, S. Heo, S. Ji, F. Bien, J.U. Park, Transparent and flexible fingerprint sensor array with multiplexed detection of tactile pressure and skin temperature, Nat. Commun. 9 (2018) 1–10, https://doi.org/10.1038/s41467-018-04906-1.
[41] L. Dhakar, S. Gudla, X. Shan, Z. Wang, F.E.H. Tay, C.H. Heng, C. Lee, Large scale triboelectric nanogenerator and self-powered pressure sensor array using low cost roll-to-roll UV embossing, Sci. Rep. 6 (2016) 1–10, https://doi.org/10.1038/srep22253.
[42] J.C. Yang, J. Mun, S.Y. Kwon, S. Park, Z. Bao, S. Park, Electronic skin: recent progress and future prospects for skin-attachable devices for health monitoring, robotics, and prosthetics, Adv. Mater. 31 (2019) 1–50, https://doi.org/10.1002/adma.201904765.
[43] C. Wang, L. Dong, D. Peng, C. Pan, Tactile sensors for advanced intelligent systems, Adv. Intell. Syst. 1 (2019), 1900090, https://doi.org/10.1002/aisy.201900090.
[44] K. Keum, J. Eom, J.H. Lee, J.S. Heo, S.K. Park, Y.H. Kim, Fully-integrated wearable pressure sensor array enabled by highly sensitive textile-based capacitive ionotronic devices, Nano Energy 79 (2021), 105479, https://doi.org/10.1016/j.nanoen.2020.105479.
[45] M. Zhu, T. He, C. Lee, Technologies toward next generation human machine interfaces: From machine learning enhanced tactile sensing to neuromorphic sensory systems, Appl. Phys. Rev. 7 (2020), 031305, https://doi.org/10.1063/5.0016485.
[46] M. Zhu, Z. Yi, B. Yang, C. Lee, Making use of nanoenergy from human – nanogenerator and self-powered sensor enabled sustainable wireless IoT sensory systems, Nano Today 36 (2021), 101016, https://doi.org/10.1016/j.nantod.2020.101016.
[47] L. Xiang, X. Zeng, F. Xia, W. Jin, Y. Liu, Y. Hu, Recent advances in flexible and stretchable sensing systems: from the perspective of system integration, ACS Nano 14 (2020) 6449–6469, https://doi.org/10.1021/acsnano.0c01164.
[48] J.R.C. Smirnov, A. Sousaraei, M.R. Osorio, S. Casado, J.J. Hernández, L. Wu, Q. Zhang, R. Xia, D. Granados, R. Wannemacher, I. Rodriguez, J. Cabanillas-Gonzalez, Flexible distributed feedback lasers based on nanoimprinted cellulose diacetate with efficient multiple wavelength lasing, Npj Flex. Electron. 3 (2019) 17, https://doi.org/10.1038/s41528-019-0062-4.
[49] A. Lund, K. Rundqvist, E. Nilsson, L. Yu, B. Hagström, C. Müller, Energy harvesting textiles for a rainy day: woven piezoelectrics based on melt-spun PVDF microfibres with a conducting core, Npj Flex. Electron. 2 (2018) 9, https://doi.org/10.1038/s41528-018-0022-4.
[50] E. Torres Alonso, D.P. Rodrigues, M. Khetani, D.-W. Shin, A. De Sanctis, H. Joulie, I. de Schrijver, A. Baldycheva, H. Alves, A.I.S. Neves, S. Russo, M.F. Craciun, Graphene electronic fibres with touch-sensing and light-emitting functionalities for smart textiles, Npj Flex. Electron. 2 (2018) 25, https://doi.org/10.1038/s41528-018-0040-2.
[51] K. Dong, X. Peng, Z.L. Wang, Fiber/fabric-based piezoelectric and triboelectric nanogenerators for flexible/stretchable and wearable electronics and artificial intelligence, Adv. Mater. 32 (2020), 1902549, https://doi.org/10.1002/adma.201902549.
[52] D. Jiang, B. Shi, H. Ouyang, Y. Fan, Z.L. Wang, Z. Li, Emerging implantable energy harvesters and self-powered implantable medical electronics, ACS Nano 14 (2020) 6436–6448, https://doi.org/10.1021/acsnano.9b08268.
[53] J. Tao, M. Dong, L. Li, C. Wang, J. Li, Y. Liu, R. Bao, C. Pan, Real-time pressure mapping smart insole system based on a controllable vertical pore dielectric layer, Microsyst. Nanoeng. 6 (2020) 1–10, https://doi.org/10.1038/s41378-020-0171-1.
[54] A. Haroun, X. Le, S. Gao, B. Dong, T. He, Z. Zhang, F. Wen, S. Xu, C. Lee, Progress in micro/nano sensors and nanoenergy for future AIoT-based smart home applications, Nano Express 2 (2021), 022005, https://doi.org/10.1088/2632-959x/abf3d4.
[55] J. Zhu, M. Cho, Y. Li, T. He, J. Ahn, J. Park, T.L. Ren, C. Lee, I. Park, Machine learning-enabled textile-based graphene gas sensing with energy harvesting-assisted IoT application, Nano Energy 86 (2021), 106035, https://doi.org/10.1016/j.nanoen.2021.106035.
[56] H. Wang, J. Zhu, T. He, Z. Zhang, C. Lee, Programmed-triboelectric nanogenerators—a multi-switch regulation methodology for energy manipulation, Nano Energy 78 (2020), 105241, https://doi.org/10.1016/j.nanoen.2020.105241.
[57] F. Wen, T. He, H. Liu, H.Y. Chen, T. Zhang, C. Lee, Advances in chemical sensing technology for enabling the next-generation self-sustainable integrated wearable system in the IoT era, Nano Energy 78 (2020), 105155, https://doi.org/10.1016/j.nanoen.2020.105155.
[58] Q. Shi, B. Dong, T. He, Z. Sun, J. Zhu, Z. Zhang, C. Lee, Progress in wearable electronics/photonics—moving toward the era of artificial intelligence and internet of things, InfoMat 2 (2020) 1131–1162, https://doi.org/10.1002/inf2.12122.
[59] J. Zhu, M. Zhu, Q. Shi, F. Wen, L. Liu, B. Dong, A. Haroun, Y. Yang, P. Vachon, X. Guo, T. He, C. Lee, Progress in TENG technology—a journey from energy harvesting to nanoenergy and nanosystem, EcoMat 2 (2020) 1–45, https://doi.org/10.1002/eom2.12058.
[60] Z. Zhao, Q. Huang, C. Yan, Y. Liu, X. Zeng, X. Wei, Y. Hu, Z. Zheng, Machine-washable and breathable pressure sensors based on triboelectric nanogenerators enabled by textile technologies, Nano Energy 70 (2020), 104528, https://doi.org/10.1016/j.nanoen.2020.104528.
[61] Z. Zhang, T. He, M. Zhu, Z. Sun, Q. Shi, J. Zhu, B. Dong, M.R. Yuce, C. Lee, Deep learning-enabled triboelectric smart socks for IoT-based gait analysis and VR applications, Npj Flex. Electron. 4 (2020) 29, https://doi.org/10.1038/s41528-020-00092-7.
[62] L. Zhao, H. Li, J. Meng, Z. Li, The recent advances in self-powered medical information sensors, InfoMat 2 (2020) 212–234, https://doi.org/10.1002/inf2.12064.
[63] H. Ouyang, D. Jiang, Y. Fan, Z.L. Wang, Z. Li, Self-powered technology for next-generation biosensor, Sci. Bull. 66 (2021) 1709–1712, https://doi.org/10.1016/j.scib.2021.04.035.
[64] F. He, X. You, H. Gong, Y. Yang, T. Bai, W. Wang, W. Guo, X. Liu, M. Ye, Stretchable, biocompatible, and multifunctional silk fibroin-based hydrogels toward wearable strain/pressure sensors and triboelectric nanogenerators, ACS Appl. Mater. Interfaces 12 (2020) 6442–6450, https://doi.org/10.1021/acsami.9b19721.
[65] D. Yang, H. Guo, X. Chen, L. Wang, P. Jiang, W. Zhang, L. Zhang, Z.L. Wang, A flexible and wide pressure range triboelectric sensor array for real-time pressure detection and distribution mapping, J. Mater. Chem. A 8 (2020) 23827–23833, https://doi.org/10.1039/d0ta08223f.
[66] L. Lin, Y. Xie, S. Wang, W. Wu, S. Niu, X. Wen, Z.L. Wang, Triboelectric active sensor array for self-powered static and dynamic pressure detection and tactile imaging, ACS Nano 7 (2013) 8266–8274, https://doi.org/10.1021/nn4037514.
[67] Y.C. Lai, J. Deng, R. Liu, Y.C. Hsiao, S.L. Zhang, W. Peng, H.M. Wu, X. Wang, Z. L. Wang, Actively perceiving and responsive soft robots enabled by self-powered, highly extensible, and highly sensitive triboelectric proximity- and pressure-sensing skins, Adv. Mater. 30 (2018) 1–12, https://doi.org/10.1002/adma.201801114.
[68] J. Xiong, P. Cui, X. Chen, J. Wang, K. Parida, M.F. Lin, P.S. Lee, Skin-touch-actuated textile-based triboelectric nanogenerator with black phosphorus for durable biomechanical energy harvesting, Nat. Commun. 9 (2018) 1–9, https://doi.org/10.1038/s41467-018-06759-0.
[69] X. Liu, P. Cui, J. Wang, W. Shang, S. Zhang, J. Guo, G. Gu, B. Zhang, G. Cheng, Z. Du, A robust all-inorganic hybrid energy harvester for synergistic energy collection from sunlight and raindrops, Nanotechnology 32 (2021), https://doi.org/10.1088/1361-6528/abb84b.
[70] J. Wang, P. Cui, J. Zhang, Y. Ge, X. Liu, N. Xuan, G. Gu, G. Cheng, Z. Du, A stretchable self-powered triboelectric tactile sensor with EGaIn alloy electrode for ultra-low-pressure detection, Nano Energy 89 (2021), 106320, https://doi.org/10.1016/j.nanoen.2021.106320.
[71] W. Zhang, L. Deng, L. Yang, P. Yang, D. Diao, P. Wang, Z.L. Wang, Multilanguage-handwriting self-powered recognition based on triboelectric nanogenerator enabled machine learning, Nano Energy 77 (2020), 105174, https://doi.org/10.1016/j.nanoen.2020.105174.
[72] M.H. Syu, Y.J. Guan, W.C. Lo, Y.K. Fuh, Biomimetic and porous nanofiber-based hybrid sensor for multifunctional pressure sensing and human gesture identification via deep learning method, Nano Energy 76 (2020), 105029, https://doi.org/10.1016/j.nanoen.2020.105029.
[73] T. Jin, Z. Sun, L. Li, Q. Zhang, M. Zhu, Z. Zhang, G. Yuan, T. Chen, Y. Tian, X. Hou, C. Lee, Triboelectric nanogenerator sensors for soft robotics aiming at digital twin applications, Nat. Commun. 11 (2020) 5381, https://doi.org/10.1038/s41467-020-19059-3.
[74] Z. Sun, M. Zhu, Z. Zhang, Z. Chen, Q. Shi, X. Shan, R.C.H. Yeow, C. Lee, Artificial Intelligence of Things (AIoT) enabled virtual shop applications using self-powered sensor enhanced soft robotic manipulator, Adv. Sci. 8 (2021), 2100230, https://doi.org/10.1002/advs.202100230.
[75] T. He, H. Wang, J. Wang, X. Tian, F. Wen, Q. Shi, J.S. Ho, C. Lee, Self-sustainable wearable textile nano-energy nano-system (NENS) for next-generation healthcare applications, Adv. Sci. (Weinh.) 6 (2019), 1901437, https://doi.org/10.1002/advs.201901437.
[76] Q. Zhang, Z. Zhang, Q. Liang, Q. Shi, M. Zhu, C. Lee, All in one, self-powered bionic artificial nerve based on a triboelectric nanogenerator, Adv. Sci. 2004727 (2021) 1–13, https://doi.org/10.1002/advs.202004727.
[77] P. Hougne, M.F. Imani, A.V. Diebold, R. Horstmeyer, D.R. Smith, Learned integrated sensing pipeline: reconfigurable metasurface transceivers as trainable physical layer in an artificial neural network, Adv. Sci. (Weinh.) 7 (2020), 1901913, https://doi.org/10.1002/advs.201901913.
[78] J. Wang, Y. Chen, S. Hao, X. Peng, L. Hu, Deep learning for sensor-based activity recognition: a survey, Pattern Recognit. Lett. 119 (2019) 3–11, https://doi.org/10.1016/j.patrec.2018.02.010.

[79] Y. LeCun, Y. Bengio, G. Hinton, Deep learning, Nature 521 (2015) 436–444, https://doi.org/10.1038/nature14539.
[80] M. Syafrudin, G. Alfian, N. Fitriyani, J. Rhee, Performance analysis of IoT-based sensor, big data processing, and machine learning model for real-time monitoring system in automotive manufacturing, Sensors (Basel, Switzerland) 18 (2018) 2946, https://doi.org/10.3390/s18092946.
[81] J. Koutník, K. Greff, F. Gomez, J. Schmidhuber, A clockwork RNN, 31st Int. Conf. Mach. Learn. ICML 2014. 5, 2014: 3881–3889.
[82] D. Lee, M. Lim, H. Park, Y. Kang, J.S. Park, G.J. Jang, J.H. Kim, Long short-term memory recurrent neural network-based acoustic model using connectionist temporal classification on a large-scale training corpus, China Commun. 14 (2017) 23–31, https://doi.org/10.1109/CC.2017.8068761.
[83] A. Graves, J. Schmidhuber, Framewise phoneme classification with bidirectional LSTM networks, Proc. Int. Jt. Conf. Neural Netw. 4 (2005) 2047–2052, https://doi.org/10.1109/IJCNN.2005.1556215.
[84] F. Wen, Z. Sun, T. He, Q. Shi, M. Zhu, Z. Zhang, L. Li, T. Zhang, C. Lee, Machine learning glove using self-powered conductive superhydrophobic triboelectric textile for gesture recognition in VR/AR applications, Adv. Sci. 7 (2020) 1–15, https://doi.org/10.1002/advs.202000261.
[85] G. Zhao, J. Yang, J. Chen, G. Zhu, Z. Jiang, X. Liu, G. Niu, Z.L. Wang, B. Zhang, Keystroke dynamics identification based on triboelectric nanogenerator for intelligent keyboard using deep learning method, Adv. Mater. Technol. 4 (2019), 1800167, https://doi.org/10.1002/admt.201800167.
[86] P. Jiao, Emerging artificial intelligence in piezoelectric and triboelectric nanogenerators, Nano Energy 88 (2021), 106227, https://doi.org/10.1016/j.nanoen.2021.106227.
[87] Y. Zhou, M. Shen, X. Cui, Y. Shao, L. Li, Y. Zhang, Triboelectric nanogenerator based self-powered sensor for artificial intelligence, Nano Energy 84 (2021), 105887, https://doi.org/10.1016/j.nanoen.2021.105887.
[88] W. Zhang, L. Deng, L. Yang, P. Yang, D. Diao, P. Wang, Z.L. Wang, Multilanguage-handwriting self-powered recognition based on triboelectric nanogenerator enabled machine learning, Nano Energy 77 (2020), 105174, https://doi.org/10.1016/j.nanoen.2020.105174.
[89] A. Ahmed, I. Hassan, J. Zu, Design guidelines of stretchable pressure sensors-based triboelectrification, Adv. Eng. Mater. 20 (2018), 1700997, https://doi.org/10.1002/adem.201700997.
[90] W. Yang, X. Wang, H. Li, J. Wu, Y. Hu, Z. Li, H. Liu, Fundamental research on the effective contact area of micro-/nano-textured surface in triboelectric nanogenerator, Nano Energy 57 (2019) 41–47, https://doi.org/10.1016/j.nanoen.2018.12.029.
[91] B.C.K. Tee, A. Chortos, R.R. Dunn, G. Schwartz, E. Eason, Z. Bao, Tunable flexible pressure sensors using microstructured elastomer geometries for intuitive electronics, Adv. Funct. Mater. 24 (2014) 5427–5434, https://doi.org/10.1002/adfm.201400712.
[92] J. Luo, Z.L. Wang, Recent progress of triboelectric nanogenerators: from fundamental theory to practical applications, EcoMat 2 (2020) 1–22, https://doi.org/10.1002/eom2.12059.
[93] R. Zhang, H. Olin, Material choices for triboelectric nanogenerators: a critical review, EcoMat 2 (2020) 1–13, https://doi.org/10.1002/eom2.12062.
[94] R.S. Ganesh, H. Yoon, S. Kim, Recent trends of biocompatible triboelectric nanogenerators toward self-powered e-skin, EcoMat 2 (2020) 1–12, https://doi.org/10.1002/eom2.12065.
[95] H. Yang, F.R. Fan, Y. Xi, W. Wu, Design and engineering of high-performance triboelectric nanogenerator for ubiquitous unattended devices, EcoMat 3 (2021) 1–36, https://doi.org/10.1002/eom2.12093.
[96] R. Zhang, M. Hummelgård, J. Örtegren, Y. Yang, H. Andersson, E. Balliu, N. Blomquist, M. Engholm, M. Olsen, Z.L. Wang, H. Olin, Sensing body motions based on charges generated on the body, Nano Energy 63 (2019), 103842, https://doi.org/10.1016/j.nanoen.2019.06.038.
[97] Y. Han, F. Yi, C. Jiang, K. Dai, Y. Xu, X. Wang, Z. You, Self-powered gait pattern-based identity recognition by a soft and stretchable triboelectric band, Nano Energy 56 (2019) 516–523, https://doi.org/10.1016/j.nanoen.2018.11.078.
[98] T. He, Q. Shi, H. Wang, F. Wen, T. Chen, J. Ouyang, C. Lee, Beyond energy harvesting – multi-functional triboelectric nanosensors on a textile, Nano Energy 57 (2019) 338–352, https://doi.org/10.1016/j.nanoen.2018.12.032.
[99] J. Yun, I. Kim, M. Ryoo, Y. Kim, S. Jo, D. Kim, Paint based triboelectric nanogenerator using facile spray deposition towards smart traffic system and security application, Nano Energy 88 (2021), 106236, https://doi.org/10.1016/j.nanoen.2021.106236.
[100] J. Yun, N. Jayababu, D. Kim, Self-powered transparent and flexible touchpad based on triboelectricity towards artificial intelligence, Nano Energy 78 (2020), 105325, https://doi.org/10.1016/j.nanoen.2020.105325.
[101] W. Zhang, L. Deng, L. Yang, P. Yang, D. Diao, P. Wang, Z.L. Wang, Multilanguage-handwriting self-powered recognition based on triboelectric nanogenerator enabled machine learning, Nano Energy 77 (2020), 105174, https://doi.org/10.1016/j.nanoen.2020.105174.
[102] M. Khorsand, J. Tavakoli, H. Guan, Y. Tang, Artificial intelligence enhanced mathematical modeling on rotary triboelectric nanogenerators under various kinematic and geometric conditions, Nano Energy 75 (2020), 104993, https://doi.org/10.1016/j.nanoen.2020.104993.

Zixuan Zhang received his B.Eng. degree from the School of Mechanical and Electrical Engineering at the University of Electronic Science and Technology of China (UESTC), Chengdu, China, in 2018. After that he received his M.Sc degree from Department of Electrical and Computer Engineering at National University of Singapore in 2019. He is currently pursuing his Ph.D at ECE, NUS. His research interests are focused on energy harvesters, self-powered sensors and triboelectric nanogenerator.

Qiongfeng Shi received his B.Eng. degree from Department of Electronic Engineering and Information Science at University of Science and Technology of China in 2012 and Ph.D. degree from Department of Electrical and Computer Engineering at National University of Singapore in 2018. He is currently a Research Fellow in the Dept. of ECE, NUS. His research interests are focused on energy harvesters and self-powered sensors.

Tianyiyi He received her B.Eng. degree from the School of Microelectronics and Solid-state Electronics at the University of Electronic Science and Technology of China (UESTC), Chengdu, China, in 2016, and has receives the Ph.D. degree from Department of Electrical and Computer Engineering at the National University of Singapore in 2020. She is currently a Research Fellow in the Dept. of ECE, NUS. Her research interests are focused on flexible electronics, wearable energy harvesters, and self-powered sensors.

Xinge Guo received his Bachelor of Engineering degree in microelectronics engineering from Southern University of Science and Technology, China, in 2019. He is currently pursuing his Ph.D at the Department of Electrical and Computer Engineering of National University of Singapore. His research interests include Energy Harvesting and Self-powered Sensor Technologies for IoT Applications.

Bowei Dong received the B.S. degree in physics with second major in mathematics from Nanyang Technological University, Singapore, in 2015, the Ph.D. degree from the NUS Graduate School for Integrative Sciences and Engineering at the National University of Singapore, Singapore, in 2019. His research interests include optical waveguides, integrated silicon photonics, and integrated mid-infrared photonics for sensing and healthcare applications.

Chengkuo Lee received his Ph.D. degree in Precision Engineering from The University of Tokyo in 1996. Currently, he is the director of Center for Intelligent Sensors and MEMS, and the GlobalFoundries Chair Professor at National University of Singapore, Singapore. In 2001, he cofounded Asia Pacific Microsystems, Inc., where he was the Vice President. From 2006–2009, he was a Senior Member of the Technical Staff at the Institute of Microelectronics, A-STAR, Singapore. He has contributed to more than 400 peer-reviewed international journal articles.